Expedited Amplitude and Phase Tolerance Analysis of Reflector Antenna Systems with Vector Spherical Waves

Pedro Robustillo, Juan Córcoles, *Senior Member*, and Jesús Rubio

***Abstract*— This work presents relevant advantages of analyzing a complete reflector antenna system based on *(i)* the expansion of the feed radiated field in terms of vector spherical waves (VSWs), and *(ii)* the characterization of the reflector domain with VSWs. It requires that the reflector be initially analyzed under the illumination of each single VSW. The output of each of these analyses is the radiated field of the reflector for each VSW excitation. Then, the accurate response of the complete antenna system, both in amplitude and phase, can be directly obtained by just linear combination of these individual-VSW-excited radiated fields, weighted by the feed transmission vector that relates the coefficients of the VSW expansions for the feeder with its input excitation mode. Thanks to the orthogonality of the VSWs, and the applicability of the far-field approximation, it turns into a very efficient approach for the whole end-to-end analysis, adding useful capabilities and flexibility for the expedited assessment of tolerances.**

***Index Terms*— Earth Observation, FEM, MoM, physical optics, RADAR, radiometers, spherical waves.**

I. Introduction

Reflector antennas have been ubiquitous in microwave and electromagnetics (EM) since the early days of electrical engineering [1-3]. For their characterization, one can highlight the good correlation of their main performance parameters (directivity, 3dB beam-width, etc.) against their approximate analysis by ray-like, geometric optics (GO). In this sense, a reflector antenna is made up of two distinct elements: a feeder and a reflector, whose interaction is considered to be negligible (so-called *far-field approximation*).

Since the last decades of the 20th century, asymptotic approximations of the Maxwell equations, such as Physical Optics (PO), or General Theory of Diffraction (GTD) have been feasible on computers, and have begun to be available on commercial software [4]. These methods offer a qualitative improvement in the prediction capabilities of a reflector excited by a feed far-field compared to GO. In fact, they are very popular and widely used nowadays for reflector analysis.

In the last years, further improvement on computer capabilities has allowed the implementation of efficient codes for the Method of Moments (MoM) including acceleration techniques in commercial software, [5][6]. MoM is a full-wave implementation of Maxwell equations and, hence, can offer trustful predictions for any arbitrary metallic geometry, at a higher computational cost.

Feeders can also be analyzed by MoM. However, smaller, detailed geometries –such as patch antennas or printed antennas– are better suited for field-based methods, such as the Finite Element Method (FEM). Also, the mode-matching method (MM) can be used in some cases [7].

From the far-field approach (where the feed far-field is used as the excitation for the analysis of the reflector to obtain the response of the complete antenna system) the following drawbacks arise: *(i)* a modification of any parameter on the feeder implies two new EM simulations: one for the feeder and another one for the reflector; *(ii)* any change of the reflector implies a further EM simulation. To cope with these two drawbacks, approximate methods have been developed in the past, most of them based on ray-like corrections, and mathematical interpolation schemes [8] [9].

In contrast, the approach in this work sets up an innovative implementation, based on the characterization of the reflector radiation by VSWs. The use of VSWs was presented in the literature years ago, for the modeling of feeders (for both analyzed [10] and measured [11] radiation patterns), providing more stability and accuracy in the mathematical resolution. Furthermore, the use of VSWs on feeders has demonstrated added capabilities, such as analytical translations and rotations [12][13], or analysis of finite arrays with mutual couplings [14]. Also, in [15] the feeder mismatch because of its interaction with the reflector is studied by projection of the reflector scattering onto a representative set of VSWs.

In this work, the use of VSWs for the characterization of radiated fields is considered not only for the feeder but also for the reflector of any arbitrary shape. This latter characterization is the most time-demanding part of the approach (~ hours), but it is done only once and can be used extensively along the complete life-cycle of the reflector design, being able of generating the sharp EM response of the complete antenna system after the change of some design parameters (for instance, feeder position and feeder change, reflector tilts, reflector deformation) in a matter a seconds.

Section II describes the theoretical background of the method. Section III contains the selected examples, including: translation and rotation of the feeder, tilt of the reflector, and reflector modifications. Finally, Conclusions will be drawn.

II. Reflector Characterization by Means of VSWs

The basis behind this approach is sketched in Fig. 1-*Left*. The reflector antenna is decomposed into two domains: the feeder and the reflector. The feeder is supposed to be enclosed inside a sphere S of radius r centered at the global coordinate system OXYZ. Then, it is analyzed, providing its radiated field $\boldsymbol{E}^{feed,rad}$, which is, in turn, projected onto q orthogonal VSWs [11], $\boldsymbol{E}^{out}{}_{SW,i}$, yielding the transmission vector $\boldsymbol{b}_{sph}$. The relation between q and r is set by [16]:

$$n = \left[kr + 0.045\sqrt[3]{kr}\,(-Ptr\,)\right] \quad (1)$$

This work was supported by the Spanish Government under grants TED2021-130650B-C21 (ANT4CLIM), PID2020-116968RB-C32 (DEWICOM) and PID2021-122856NB-C21, funded by MCIN/AEI/ 10.13039/501100011033 (Agencia Estatal de Investigación), by UE (European Union) "NextGenerationEU"/PRTR and by ERDF A Way of making Europe (FEDER, UE).

P. Robustillo works as Elec. & Electronic Developt. Responsible at TSEIM1-TL3, AIRBUS, Germany (e-mail: pedro.robustillo@airbus.com).

J. Córcoles is with Escuela Politécnica Superior (School of Engineering), Universidad Autónoma de Madrid, Spain (e-mail: juan.corcoles@uam.es).

J. Rubio is with Escuela Politécnica, Universidad de Extremadura, Cáceres, Spain (e-mail: jesusrubio@unex.es).

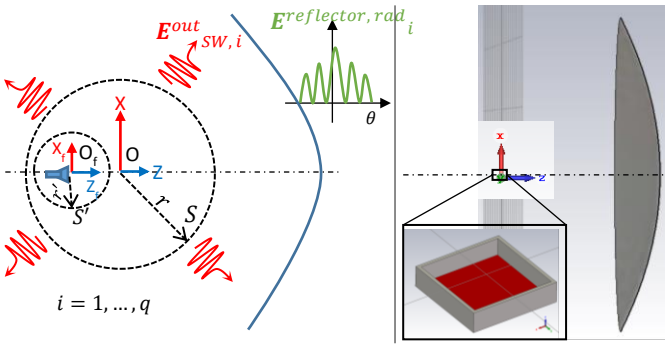

Fig. 1. *Left:* Sketch of a reflector characterized by VSWs. *Right:* Circular parabolic reflector. Radius: 20λ; focal distance: 20λ; focal point F (0,0,0) mm. Feeder: $0.6\lambda \times 0.6\lambda \times 0.1\lambda$ square waveguide.

where k is the wavenumber, Ptr is the relative power of the feed radiation pattern that is neglected, and n is the degree of the VSWs, linked to the number of modes q by:

$$q = 2 \cdot n \cdot (n+2) \tag{2}$$

Then, the feed radiated field can be reconstructed as:

$$\boldsymbol{E}^{feed,rad} = \sum_{i=1}^{q} b_{sph,i}\, \boldsymbol{E}^{out}{}_{SW,i} \tag{3}$$

Now, rather than using $\boldsymbol{E}^{feed,rad}$ as the excitation for the reflector, q individual analyses of the reflector will be done, each of which with one of the q VSWs as excitation, according to the coordinate system OXYZ. The output of each analysis is the reflector radiated field $\boldsymbol{E}_i^{reflector,rad}$ with respect to OXYZ.

Then, the radiation pattern of the complete antenna can be directly obtained as:

$$\boldsymbol{E}^{total,rad} = \sum_{i=1}^{q} b_{sph,i}\, \boldsymbol{E}_i^{reflector,rad} \tag{4}$$

since the coefficient of the each VSW radiated by the feeder becomes the excitation of the homologous VSW in the reflector characterization, thanks to the orthogonality of the VSWs.

From an equivalent point of view, a feeder in this context is any electromagnetic geometry whose minimum enclosing sphere, S', of radius r', centered at its own reference system, $O_fX_fY_fZ_f$, lies inside the virtual sphere S. This interpretation opens the door to consider the application of the VSW addition theorems to account for rotations and translations of the feeder [11]. For this, the feed radiated field is projected onto p VSWs, defined according to its local coordinate system $O_fX_fY_fZ_f$, where p and r' fulfill (1) and (2) above, yielding $p \leq q$.

Then, the feed transmission vector of the rotated-translated feeder, $\boldsymbol{b}_{sph}{}^{rot-trans}$, with respect to OXYZ, can be obtained as:

$$\boldsymbol{b}_{sph}{}^{rot-trans} = \boldsymbol{G}\, \boldsymbol{b}_{sph,min} \tag{5}$$

where $\boldsymbol{b}_{sph,min}$ is the $p \times 1$ transmission vector of the feeder in its own local coordinate system, $O_fX_fY_fZ_f$, and $\boldsymbol{G}$ is a $q \times p$ matrix that accounts for rotations and translations (second case of addition theorems in [11]). As a consequence, $\boldsymbol{G}$ will properly model any translation of vector $\overrightarrow{OO_f}$ with respect to OXYZ provided S' still lies inside S, after application of $\overrightarrow{OO_f}$ (see Fig.1-*Left*).

On the other hand, once the q-VSW characterization of the reflector is obtained, it can be also useful to quickly assess the impact of a modification of the reflector surface, as explained next.

With regard to the radiation field of the feeder, (3), it is well-known that the following approximation for the field amplitude holds inside the far-field region, [1]:

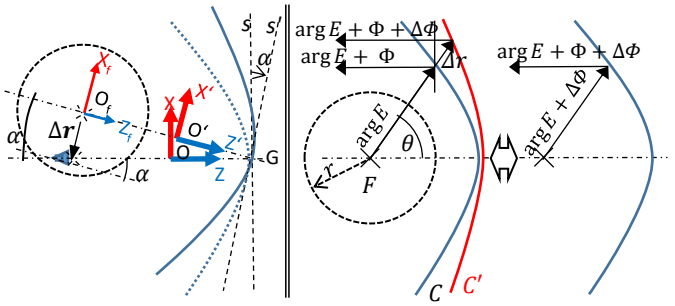

Fig. 2. *Left:* Sketch of Reflector Tilt by angle α, around point G. *Right:* Sketch of generation of *equivalent* feed radiation pattern under a reflector-surface modification in the far-field region.

$$|\boldsymbol{E}(\boldsymbol{r})| \approx |\boldsymbol{E}(\boldsymbol{r} + \Delta\boldsymbol{r})|, \quad |\Delta\boldsymbol{r}| \ll |\boldsymbol{r}| \tag{6}$$

where $|\cdot|$ stands for the amplitude value, $\boldsymbol{r} = \boldsymbol{r}(r, \theta, \varphi)$ is the position vector of a point in the far-field region, and $\Delta\boldsymbol{r}$ is a relative position vector with respect to $\boldsymbol{r}$.

Now, let us consider the situation depicted in Fig. 2- *Right*. There is a nominal reflector C (whose characterization in terms of VSWs is known) and a modified reflector C'. At an angle θ (φ omitted for clarity), C' adds a $\Delta\boldsymbol{r}$ in the propagation path of the feed radiation pattern which, in turns, generates a $\Delta\Phi$ in the phase Φ of the reflected field as:

$$\Delta\Phi = \frac{2\pi}{\lambda}\Delta r(1 + cos\theta) \tag{7}$$

Therefore, if the phase of the feed field at θ, $\arg \boldsymbol{E}$, was pre-processed according to:

$$\arg \boldsymbol{E}' = \arg \boldsymbol{E} + \Delta\Phi \tag{8}$$

and this phase-modified feed field, $\boldsymbol{E}'$, was used to feed C, the resulting pattern of the complete system would be approximately equivalent to the one generated by the nominal feeder and C', Fig. 2-*Right*. This approximation can be accepted as long as the condition (6) for the far-field of the feeder is satisfied, which can be established as:

$$||\,|\boldsymbol{E}(\boldsymbol{r})| - |\boldsymbol{E}(\boldsymbol{r} + \Delta\boldsymbol{r})|\,|| < \delta\,, \forall(\theta, \varphi) \in \partial S_{ref} \tag{9}$$

where ∂S_{ref} is the solid angle over the reflector, and the value of δ is a problem-dependent parameter to be defined according to the difference found in the complete antenna radiation pattern between a reference EM method and this work (as shown in Section III.C).

Then, to profit from the q-VSW characterization of C, the pre-processed feed field $\boldsymbol{E}'$ can be projected onto these q VSWs, yielding the transmission vector $\boldsymbol{b}_{sph}$, which can be used to obtain the radiation pattern of the complete system with (4), achieving a good approximation of the reflector antenna made up of the nominal feeder and the modified reflector C' with very little computational cost compared to repeating the analysis of the whole antenna system.

III. Application Cases

A. Reference demonstrator

A parabolic reflector of radius 20λ and focal distance 20λ at 5GHz has been selected (see Fig. 1-*Right*) defined as:

$$\begin{cases} x = r \cdot \cos(\varphi)\,, r \in [0{,}1200]\, mm \\ y = r \cdot \sin(\varphi)\,, \ \varphi \in [0°, 360°] \\ z = (-2.0833 \cdot 10^{-4}) \cdot r^2 + 1200 \end{cases} \tag{10}$$

This geometry and this operation frequency are representative of, for instance, those of space SAR and lower-frequency radiometers, [17], [18]. For this demonstrator, a section of square waveguide, $0.6\lambda \times 0.6\lambda \times 0.1\lambda$, has been considered as feeder (Fig. 1-*Right*).

Coordinate systems for feeder and reflector radiation patterns are the same, centered at the focal point $F(0,0,0)$. The feeder fits inside a virtual sphere, S', of radius $r' = 0.5\lambda$. From (2), p for the feeder should be 70 (for a neglected relative power, Ptr, of $-65dB$), and so could be q for the reflector. However, thinking on future uses, up to 510 reflector VSWs ($q = 510$) were considered ($n = 15$, according to (2)), which allows a virtual sphere, S, of radius $r < 0.9\lambda$ for the allocation of the feeder, and $Ptr = -90\ dB$. The duration of each VSW-reflector analysis by MoM [5] took about 350 s on an Intel i7-6700 CPU @3.40GHz 64GB RAM, on 4 cores (out of 8 available). During this set of analyses, the radiated field of the reflector after each VSW, $\boldsymbol{E}_i^{reflector,rad}$, was stored. The analysis of the feed was also carried out by MoM [5], with a time of 10 s.

Fig. 3 shows the comparison of the radiated field obtained in this work (solid - red) vs. the radiated field computed considering the excitation of the reflector by the feed radiated field given by [5] (dash - red). An excellent agreement is found, not only in amplitude but also in phase (which is of importance in Earth Observation applications). In fact, the method in this work can also be considered as a full-wave method, in the sense that it directly implements the analysis from Maxwell equations, without any mathematical approximation, other than the far-field approximation and the truncation at (p, q). It must be pointed out that the feeder-to-reflector connection took less than 1 s.

B. *Translation and rotation of feed. Reflector tilt*

Once the reflector is characterized, the effect of translations and rotations of the feeder on the complete antenna can be accomplished straightforwardly, as explained in Section I. Fig. 3 shows also the results after application of translations to the feeder of $-15mm$ (green) and $-30\ mm$ (blue), along the X-axis. As seen, agreement with [5] is very good. At cut $\phi = 0°$, the effect of a feeder translation is clearly visible: a mispointing. Therefore, cut $\phi = 90°$ is no longer where the peak value can be found. This explains that the value at $\theta = 180°$ in this cut is not the maximum. The time needed by this approach was 0.5 s for setting the input data, <1 s to perform the translation, and 1.1 s to generate the new radiation pattern: <2.6 s per analysis (vs. *ca.* 780 s needed by [5]).

On the other hand, a reflector tilt with respect to a pivot point *G* can be also interpreted as equivalent translations and rotations of the feeder. Fig. 2-*Left* sketches this situation for a tilt of an angle α around the Y-axis (generalization for other axes is immediate). The problem is equivalent to a rotation α and a translation $\Delta\boldsymbol{r}$ of the feeder, followed by a change of coordinates of the resulting antenna radiated field from O'X'Y'Z' to OXYZ. Fig. 4 shows the results of the analyses for $\alpha = -0.5°$ (green) and $-1.0°$ (blue), $G = (0,0,1200)mm$. An excellent agreement vs. [5] is obtained, at a time-cost of only <2.7 s per analysis.

C. *Tolerance analysis: reflector surface*

The z-coordinate of the parabolic reflector defined by (10) will be modified according to:

$$\{z = (-2.0833 \cdot 10^{-4}) \cdot r^2 + 1200 + a \cdot |\sin(\varphi)| \qquad (11)$$

For $a \in \{2,3,4\}mm$. Qualitatively, this modification adds a change of the initial reflector surface, as a function of φ, up to a value of $a \in \{2,3,4\}\ mm$. This effect could be representative of, for instance, manufacturing errors, or the result of thermal gradients [19]. For this example, the reflector was also characterized by using PO [4]. Each of the PO analysis took about 48 s for a radiation pattern made up of 401×401 field points (20°×20° with steps of 0.1°, 6736 PO points).

Fig. 5 (*upper* and *mid* rows) shows the results, compared against simulation of the complete antenna with MoM [5]. As the deformation gets larger (i.e. a increases), the main beam of the complete antenna gets wider, the peak directivity gets lower, and the side lobes get higher. All these effects are found when using [5] (dash) and are very accurately reproduced by this work, for reflector characterization both with MoM [5] (solid) and PO [4] (dotted). Regarding the values around the peak, differences lower than 0.05dB are found between [5] and this work. Excellent correlation is also obtained up to $\theta = \pm 5°$ w.r.t. peak values on both cuts for $a = 2$. Differences begin for $a = \{3,4\}$ from $\theta = \pm 3°$ at cut $\phi = 90°$, where the amplitude values are, however, already *ca.* 20dB below the peak value.

The validity of this approximation can be assessed from (9) in Fig. 5-*lower*, where the two principal cuts of the reconstructed feed radiation pattern are presented for each value of a ($\partial S_{ref} = \{\theta < 55°\}$). For $a = 2$, the correlation is very good, with negligible differences. For $a = 3$, differences in the order of $\delta < 0.2$dB can be found. For $a = 4$, although differences $\delta < 0.4$dB are observed, the approximation still offers the main features of the radiated field of the complete antenna system. Therefore, $\delta = 0.4$dB could be set as maximum feed-pattern allowable change to be used in subsequent analyses of the reflector deformations, up to 4mm of deformation w.r.t. the nominal surface. The time to analyze each case of a in this work was 0.8 s for the implementation of the phase modification, and ~1 s for the connection, when using Matlab©. On the other hand, each analysis with [5] took *ca.* 780 s (i.e. a speed-up factor of $\sim 4 \cdot 10^2$).

As a final example, a similar study has been done for an offset-fed parabolic reflector of 100λ resulting after the intersection of:

$$parabol \coloneqq \begin{cases} x = r \cdot \cos(\varphi), r \in [0,6100]\ mm \\ y = r \cdot \sin(\varphi), \quad \varphi \in [0°, 360°] \\ z = (-4.1666 \cdot 10^{-5}) \cdot r^2 + 6000 + a \cdot |\sin(2\varphi)| \end{cases}$$
$$cylinder \coloneqq \{(x - 3100)^2 + y^2 \leq 3000^2 \qquad (12)$$

The reflector was characterized with PO [4], taking 88 s per analysis, for 401×401 field points (10°×10° with steps of 0.05°, 26208 PO points). The same feeder was used, with a 33° rotation along the Y-axis (implemented as in Section III.B). Results are shown in Fig. 6, where excellent agreement is observed over the main lobe, both for amplitude and phase, and all a values. The differences in side lobe values are <1dB for all cases. The time per analysis was 0.34 s for the phase modification (the reflector covers a smaller solid angle) and <0.1 s for the connection (radiation pattern of 401×401 points).

IV. Conclusion

Starting from the familiar approach of using the feed expansion into VSWs to excite a reflector, this work has elaborated a complete and fast approach for end-to-end reflector antenna analysis, capable of handling modifications of feeder and feeder position, reflector tilt, and reflector deformation. For this purpose, an extensive characterization of the reflector in terms of individual VSWs (one EM analysis per VSW) is initially needed, where the number of VSWs depends on the size of the virtual sphere, S, in which any potential feeder could be

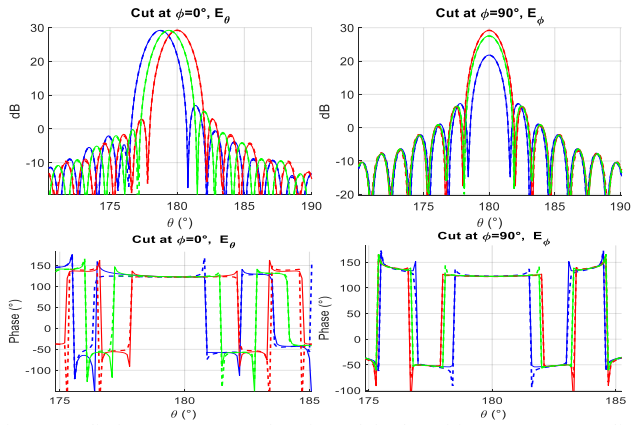

Fig. 3. Radiation pattern as a function of feed position. *Upper:* Amplitude. *Lower:* Phase. Red: Reference demonstrator. Green: feed translated to (-15, 0, 0) mm. Blue: feed translated to (-30, 0, 0) mm. Solid: this work. Dashed: [5].

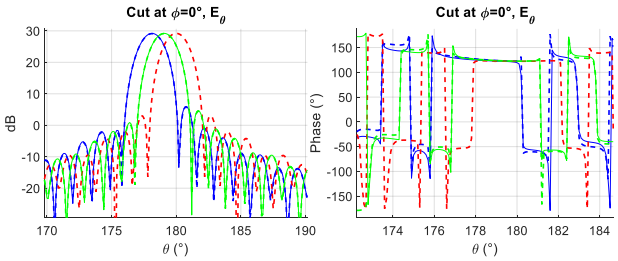

Fig. 4. Radiation pattern as a function of reflector tilt α. *Left:* Amplitude. *Right:* Phase. Green: $\alpha = -0.5°$. Blue: $\alpha = -1.0°$. G=(0,0,1200) mm. Red: reference, $\alpha = 0°$. Solid: this work. Dashed: [5].

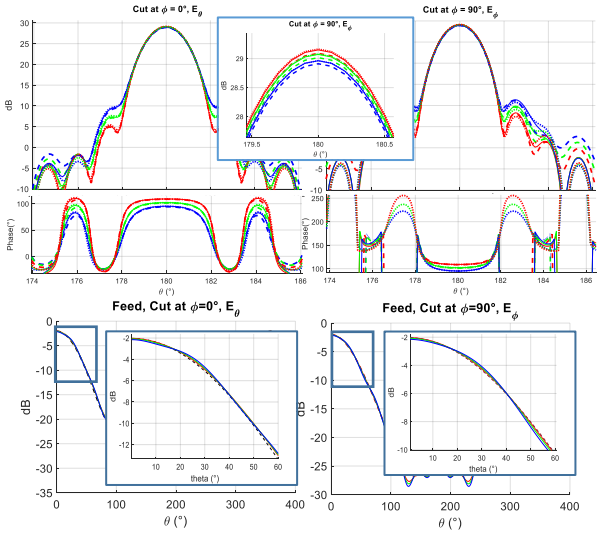

Fig. 5. *Upper-Mid:* Radiation pattern after modification of the reflector (11). $a = \{0,2,3,4\}$={black, red, green, blue}. Solid/Dotted: this work with MoM/PO. Dashed: complete antenna by MoM [5]. *Lower:* Feed radiation patterns. Solid: modified feed radiation pattern by this work $a = \{2,3,4\}$={red, green, blue}. Dashed: nominal feed radiation pattern. *Inset:* Details around peak.

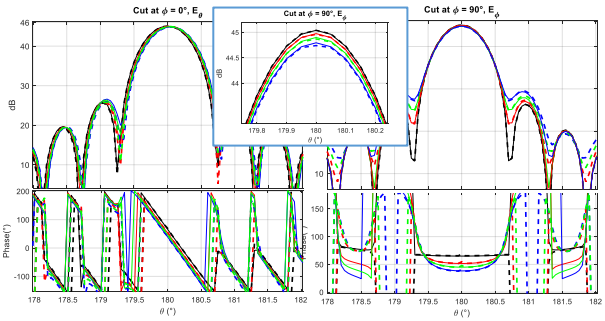

Fig. 6. Radiation pattern of the 100λ, offset-fed reflector antenna (12), $a = \{0, 2,3,4\}$={black, red, green, blue}. Solid: this work with PO [4]. Dashed: complete antenna by MoM [5]. *Inset:* Details around peak.

later included. Even if it may look prohibitive at first glance, the current capabilities of even low-medium computers allow carrying out this number of analyses within a reasonable amount of time. It must be recalled that this characterization is not restricted to any particular reflector shape and can be done with different EM methods (such as MoM or PO). Then, under the assumption of far-field excitation, the transmission vector of the feeder, $\boldsymbol{b}_{sph}$, can be computed, which can be analytically manipulated and connected to the reflector in a matter of seconds (speed-up factor ~10^2). Therefore, the initial time required for the reflector characterization is quickly returned back along the complete life-cycle of the antenna design since, for instance as shown in this work, tolerance analysis of both feeder and reflector positions can be done with a negligible time, *(i)* yielding the complete (amplitude and phase) radiated field of the whole system as the output; *(ii)* being accurate enough for even high-end applications, such as Earth Observation, where the knowledge of both the main beam and the side lobes is key to reach the required performances.

REFERENCES

[1] W. V. T. Rusch and P. D. Potter, *Analysis of Reflector Antenna*, Academic, NY, USA, 1970.

[2] A. W. Love (Ed.), *Reflector Antennas*, IEEE Press Institute of Electrical and Electronics Engineers, NY, USA, 1978

[3] P. J. Wood, *Reflector antenna analysis and design*, IEE electromagnetic waves series, Hardcover, 1980

[4] TICRA-GRASP©, https://www.ticra.com/software/grasp/

[5] CST© Microwave Studio Suite, 2018.

[6] Altair Feko, Altair Inc., Troy, Michigan, USA, 2022.

[7] J. Encinar and J. Rebollar, "Accurate analysis of feed-horns by a new hybrid modal-spectral method," in *Proc. 1985 Antennas and Propagation Society International Symposium*, 1985, pp. 331-334, doi: 10.1109/APS.1985.1149561.

[8] F. Mini et al., "European Large Deployable Antenna: Development Status and Applications," in *The Second European Conference on Antennas and Propagation*, EuCAP 2007, 2007, pp. 1-1.

[9] P. Rocca, N. Anselmi and A. Massa, "Interval Arithmetic for Pattern Tolerance Analysis of Parabolic Reflectors," *IEEE Transactions on Antennas and Propagation*, vol. 62, no. 10, pp. 4952-4960, Oct. 2014, doi: 10.1109/TAP.2014.2342758.

[10] C. Rieckmann, M. R. Rayner, C.G. Parini, "Application of UTD and Spherical Wave Theory to Reflector Antenna Analysis," in *National Conference on Antennas and Propagation*, 30, March – 1, April, 1999, Conference Publication No. 461, © IEE, 1999.

[11] J. E. Hansen, *Spherical Near Field Antenna Measurements*. Peter Peregrinus Ltd., London, U.K., 1988, pp. 47-48

[12] I. P. Kovalyov, N. I. Kuzikova, D. M. Ponomarev, "Transformation of Antenna Generalized Scattering Matrix During Rotation and Linear Displacement," *IEEE Trans. Antennas Propag*., vol.: 64 , is.: 12, pp. 5110 – 5121, Dec. 2016.

[13] P. Robustillo, J. Rubio, J. Zapata and J. R. Mosig, "Direct FEM-Domain Decomposition Using Convex-to-Concave Spherical Ports for Space Applications," *IEEE Antennas and Wireless Propagation Letters*, vol. 19, no. 12, pp. 2230-2234, Dec. 2020, doi: 10.1109/LAWP.2020.3028287.

[14] J. Rubio, M. A. González, and J. Zapata, "Generalized-scattering-matrix analysis of a class of finite arrays of coupled antennas by using 3-D FEM and spherical mode expansion," *IEEE Trans. Antennas Propag.*, vol. 53, no. 3, pp. 1133–1144, Mar. 2005.

[15] C. Della Giovampaola, E. Martini, A. Toccafondi and S. Maci, "A Hybrid PO/Generalized-Scattering-Matrix Approach for Estimating the Reflector Induced Mismatch," *IEEE Trans. Antennas Propag*., vol. 60, no. 9, pp. 4316-4325, Sept. 2012, doi: 10.1109/TAP.2012.2207062.

[16] F. Jensen and A. Frandsen, "On the number of modes in spherical wave expansions," in *Proc. 26th AMTA*, Stone Mountain Park, GA, USA, Oct. 2004, pp. 489–494.

[17] M. Sedehi, E. Imbembo, A. Carbone, F. Heliere, B. Rommen, M. Fehringer, A. Leanza, T. Simon, P. Willemsen, K. Scipal, Klaus, "Biomass - A fully polarimetric P-band SAR ESA mission," in *13th European Conference on Synthetic Aperture Radar*, EUSAR, 2021, Leipzig, Germany, 2021.

[18] C. Cappellin, J. R. de Lasson, K. Pontoppidan, N. Skou, "Multi-Feed-per-Beam Antenna Conecept for High-Performance Passive Microwave Radiometers," in *Proc. 39th ESA Antenna Workshop on Multibeam and Reconfigurable Antennas for Space Applications*, 2-4 October 2018, Noordwijk, The Netherlands.

[19] R. Sharp, M. Liao, J. Giriunas, J. Heighway, A. Lagin, R. Steinbach, "Reflector surface distortion analysis techniques (thermal distortion analysis of antennas in space)", NASA, Langley Research Center, Earth Science Geostationary Platform Technology, July, 1st, 1989. Document ID 19900009951.